https://doi.org/10.5194/egusphere-2024-2206
Preprint. Discussion started: 14 August 2024

Distinct effects of Fine and Coarse Aerosols on Microphysical Processes of Shallow Precipitation Systems in Summer over Southern China

Fengjiao Chen [1,2], YuanjianYang[3*], Lu Yu[1], Yang Li[1], Weiguang Liu [1], Yan Liu [1], Simone Lolli[4]

[1] *Key Laboratory of Transportation Meteorology of China Meteorological Administration, Nanjing Joint Institute for Atmospheric Sciences, Nanjing, China*

[2] *China Meteorological Administration Radar Meteorology Key Laboratory, Beijing, China*

[3] *School of Atmospheric Physics, Nanjing University of Information Science and Technology, Nanjing, Jiangsu, China*

[4] *CNR-IMAA, Contrada S. Loja, 85050 Tito Scalo (PZ), Italy*

**Corresponding author: Prof. Yuanjian Yang (yyj1985@nuist.edu.cn)*

https://doi.org/10.5194/egusphere-2024-2206
Preprint. Discussion started: 14 August 2024

Abstract: The densely populated South China, adjacent to the South China Sea, which is associated with shallow precipitation during summer, makes it a natural experimental region for studying the impact of aerosols on shallow precipitation events. Using 8 years of GPM DPR, MERRA-2 aerosol, and ERA reanalysis data, this study investigates the potential influence of coarse and fine aerosol modes on the precipitation structure and microphysical processes of shallow precipitation in South China. Statistical results indicate that during coarse aerosol-polluted conditions, shallow precipitation clouds have a lower median Storm Top Height (STH, ~3.2 km), but a higher mean near-surface rainfall (RR, ~1.78 mm h^{-1}), characterized by high concentrations of large raindrops, mainly driven by significant collision-coalescence processes (accounting for 74.1%). Conversely, during fine aerosol-polluted conditions, shallow precipitation clouds develop deeper median STH ~3.7 km with lower surface RR characterized by a low concentration of small hydrometeors, resulting from increased breakup processes (33.1%) and reduced collision-coalescence processes (69.6%). The coarse (fine) aerosols act as promoters (inhibitors) of the radar and radar reflectivity in the profile of shallow precipitation, regardless of dynamic and humid conditions. The effect of coarse aerosols in promoting precipitation and the inhibiting effect of fine aerosols are the most significant under low humidity conditions, mainly attributed to the significantly enhanced collision-coalescence processes, exceeding 22.2%. Furthermore, the increase in RR above 3 km during coarse aerosol-polluted environments is mainly driven by the high concentration of hydrometeors in low instability conditions, while by large hydrometeors in high instability environments.

https://doi.org/10.5194/egusphere-2024-2206
Preprint. Discussion started: 14 August 2024

Short Summary: The precipitation microphysical mechanisms responsible for the varied impacts of aerosols on shallow precipitation remain unclear. This study reveals that coarse aerosols invigorate shallow rainfall through enhanced coalescence processes, whereas fine aerosols suppress shallow rainfall via intensified breakup microphysical processes. These impacts are independent of thermodynamic environments but are more significant in low-humidity conditions.

1 Introduction

Shallow precipitation, typically classified based on the storm height, prevails over the ocean and marine continent, which could contribute 20% of the rainfall over tropical oceans and 7.5% over topical land (Liu and Zipser, 2009; Chen et al., 2016; Short and Nakamura, 2000). This underscores its crucial significance in the regulation of the global water cycle. However, shallow precipitation is a complex phenomenon influenced by various factors such as water vapor, thermodynamic environment, and aerosols (Lang et al., 2021; Chen et al., 2024; Smalley and Rapp, 2020). Among these factors, aerosols have been the subject of intense debate due to the complexity of aerosol-radiation interactions and aerosol-cloud interactions between different species, leading to unresolved questions regarding whether aerosols will enhance or suppress shallow precipitation (Koren et al., 2014; Fan et al., 2020; Christensen and Stephens, 2012).

The impact of aerosols on precipitation has been widely investigated in many previous studies (Sun and Zhao, 2021; Miltenberger et al., 2018; Liu et al., 2022; Fan et al., 2018). Regional differences show that aerosols can delay the start time of precipitation by 2 hours in the Pearl River Delta but advance by 3 hours in the North China Plain (Sun and Zhao, 2021). Furthermore, precipitation is suppressed for stratocumulus and small cumulus clouds in high aerosol environments, but enhanced for heavy precipitation events and deep convective clouds (Yuan et al., 2011; Rosenfeld et al., 2008; Xiao et al., 2022; Miltenberger et al., 2018). However, convective rainfall invigoration depends on aerosol concentrations, which turns into suppression at the turning zone of aerosol optical depth in 0.25-0.30 (Guo et al., 2019), potentially linked

https://doi.org/10.5194/egusphere-2024-2206
Preprint. Discussion started: 14 August 2024

to a change from aerosol microphysical effects to aerosol radiative effects (Jiang et al., 2016). Focusing on different aerosol species, Liu et al. (2022) found an improvement of rainfall flux for marine warm clouds by a factor of 4 in high coarse spray aerosols, but a suppression by a factor of 0.25 in high fine aerosol conditions. Additionally, these contrast effects are independent of meteorological conditions. Other studies suggest that the improvement of rainfall in orographic regions with high mineral dust concentrations is more significant in humid environments (Zhang et al., 2020b). In general, the impacts of aerosols on precipitation are determined by many factors, including meteorology, aerosol types, aerosol concentration, cloud types, and so on and therefore must be disentangled.

Most of these studies on the interactions between aerosols and precipitation have focused on the intensity, frequency of precipitation, and start and peak times of precipitation, but few studies have reported on how aerosols impact rainfall through modulating microphysical structures and processes of precipitation. Using three-dimensional observations of precipitation and microphysics from dual frequency precipitation radar (DPR) onboard the Global Precipitation Mission (GPM), recent studies have revealed that aerosol mainly reduces mean droplet concentration and increases the effective radius of precipitation in most regions of eastern China (except Northeast China) (Sun et al., 2022); Xiao et al. (2022) found that the aerosol invigoration effect on convective rainfall is characterized by higher droplet concentration with smaller size under polluted conditions in Northeast China. However, the impact of different aerosol species on precipitation microphysical structures and microphysical processes (i.e., efficiency of coalescence of rain droplets) has rarely been studied, which is crucial for understanding the complete chain of the relationships between aerosols, precipitation microphysics, and precipitation.

South China (18~29°N, 110~123°E) is a region where shallow precipitation occurs frequently (occurrence frequency up to 20%) and different types of aerosols prevail during summer (Yang et al., 2021), making it an ideal region for the study on the effect of the effect of aerosols on shallow precipitation. Using the combined data set of GPM

https://doi.org/10.5194/egusphere-2024-2206
Preprint. Discussion started: 14 August 2024

DPR and MERRA-2 (Modern-Era retrospective analysis for Research and Applications, Versions2), this study aims to answer the following questions: 1) Will the coarse and fine aerosols enhance or weaken the surface precipitation of shallow precipitation, 2) How do aerosols affect the precipitation microphysical structures or processes (i.e., break-up, collision-coalescence), 3) Are the relations between aerosols and rainfall, microphysical structures and processes sensitive to the dynamical and vapor component? The data and methods are introduced in Section 2. Section 3 discusses the impacts of fine and coarse aerosols on the microphysical properties and processes for shallow precipitation. A summary and conclusions are presented in Section 4.

2 Data and Methods

2.1 Data

In this study, four different data set are used to illustrate the potential impact of aerosols on microphysical precipitation structures and shallow precipitation processes over southern China during the summers between 2014 and 2021.

In the present study, the hourly MERRA-2 aerosol dataset (MERRA2_400.tavg1_2d_aer_Nx) at 0.5 × 0.625 spatial resolution is used. MERRA-2 is produced using the Goddard Earth Observing System, Version 5 (GEOS-5) atmospheric model and the Gridpoint Statistical Interpolation (GSI) assimilation system (Molod et al., 2015). GEOS-5 integrates a radiatively coupled version of the Goddard Chemical Aerosol Radiation and Transport (GOCART) model to simulate aerosol components (Chin et al., 2002). In the estimation of aerosol properties, MERRA-2 assimilates aerosol data from ground-based observations from Aerosol Robotic NETwork (AERONET) and spaceborne aerosol products from Advanced Very High Resolution Radiometer (AVHRR), Multiangle Imaging Spectro Radiometer (MISR) (Randles et al., 2017; Buchard et al., 2017). Aerosol species, including black carbon, organic carbon, sulfate, sea salt, and dust, are assumed to be external mixtures

https://doi.org/10.5194/egusphere-2024-2206
Preprint. Discussion started: 14 August 2024

that do not interact with each other. Previous studies have shown a relatively good consistency of AOD from MERRA-2 and ground-based observations, i.e., AERONET, Sun sky radiometer Observation NETwork (SONET) (Ou et al., 2022; Buchard et al., 2015; Sun et al., 2019a). Since MERRA-2 lacks nitrate aerosols that account for negligible parts of total aerosol concentration, it can lead to underestimations in the estimation of total AOD and fine aerosols (Sun et al., 2019b). However, using the percentile method to identify high aerosol loading conditions may reduce uncertainties caused by underestimating AOD to some extent. In this present study, we consider the aerosol optical thickness and the extinction at 550 nm for five species, i.e. black carbon, organic carbon, sulfate, sea salt, and dust, as well as the Angstrom exponent (α) between 470 and 870 nm. α is a significant parameter in aerosol science, which elucidates the AOD dependency on wavelength. A higher α is related to a higher concentration of fine particles, whereas a lower α suggests higher concentration of coarse particles(Lolli et al., 2023)

The GPM DPR consists of two precipitation radars operating in the Ka and Ku bands, providing a unique opportunity to obtain information on three-dimensional precipitation and particle drop size distributions (DSDs) at the same time. In the present study, the official 2ADPR (version 7) dataset covering the summers (June to August) of 2014 and 2021 is also used, which provides information on the observation time, near-surface rain rate (RR), liquid water path (LWP), the three-dimensional profiles of attenuation-corrected reflectivity (Z_e), rainfall, the mass-weighted mean diameter Dm (in mm) and the generalized intercept N_w (in mm^{-1} m^{-3}) of the normalized gamma distributions with a vertical resolution of 125 m in each scanning pixel (Iguchi et al., 2017). The reliability of DSDs and precipitation has been validated by many previous studies (Huang et al., 2021; Radhakrishna et al., 2016). Due to the high spatial resolution (125m in vertically and 4.5 km in horizontal resolution), the official 2ADPR (version 7) dataset has been widely used in the field of climatology (Chen et al., 2024; Zhang et al., 2020a; Chen et al., 2020). Shallow precipitation clouds are defined by their near-surface RR exceeding 0.1 mm h^{-1} and STH below 5 km in altitude. The storm

https://doi.org/10.5194/egusphere-2024-2206
Preprint. Discussion started: 14 August 2024

top height (STH) is defined as the maximum height where the Z_e exceeds 20dBZ (Liu and Zipser, 2013).

In this study, convective available potential energy (CAPE) and relative humidity (RH) at 850 hPa from the fifth generation global reanalysis of the European Center for Medium-Range Weather Forecasts (ERA5) covering the period from 2014 to 2021 are also used to investigate the meteorological dependence on the relationship between aerosols and precipitation. Additionally, the global 1km grid quality-controlled global digital elevation model (DEM) (https://ngdc.noaa.gov/mgg/topo/globe.html) is also used to exclude the influence of topography in the present study.

2.2 Methods

Due to the different spatial and temporal resolutions of DPR, MERRA-2, and ERA5, these three datasets must be matched before investigating the potential impact of different types of aerosols on shallow precipitation. Since the DPR detects the rainy pixels at approximately 4.5 km spatial resolution, both MERRA-2 at 0.5 × 0.625° resolution and ERA5 at 0.25° resolution are first linearly interpolated to 0.05° resolution. To represent the aerosol conditions before shallow precipitation, MERRA-2 AOD observations, close to DPR observation time with a spatial resolution of 0.05 ° are considered. The atmospheric data at 0.05° resolution closest to the center and the observation time of the DPR pixel are obtained from ERA5. The aerosol fine mode AOD is defined as the total AOD sum of partial AOD of black carbon, organic carbon, and sulfate, while the AOD of coarse aerosols is the total value of the sum of AOD values of sea salt and dust particles. Furthermore, to rule out the effect of topography on precipitation and aerosols, only shallow precipitation pixels that occur over a topography of less than 100 m is included in the study.

In Figure 1a, the probability density of joint distribution of AOD and α before the shallow precipitation event is represented. Shallow precipitation is most likely to occur

https://doi.org/10.5194/egusphere-2024-2206
Preprint. Discussion started: 14 August 2024

when the AOD is around 0.4 and α is around 1.4, indicating the dominance of fine aerosols. This is mainly attributed to the prevalence of fine aerosols in South China during summer, as shown in Figure 1b, where the probability density distributions (PDF) of AOD between fine aerosols and total aerosols show similar values. However, shallow precipitation also occurs in environments dominated by coarse aerosols, showing a high frequency when α is less than 1 and AOD is less than 0.3 (Figure 1a).

To classify the clean and aerosol-polluted conditions over South China, PDFs of AOD for fine, coarse and total aerosols are calculated before shallow precipitation, as shown in Figure 1b. It can be observed that the coarse mode AOD is relatively small, primarily distributed between 0 and 0.2, while fine mode AOD and total AOD are almost equal, mainly concentrated between 0 and 1.0. Specifically, the peak frequency occurs at an AOD of approximately 0.1 for coarse aerosols, 0.15 for fine aerosols, and 0.2 for total aerosols. We define a clean environment as one in which the AOD of the total aerosols fall below the 30th percentile in all the data sampled, specifically the AOD of the total aerosols < 0.025 (see Table 1 for reference). A fine aerosol-polluted environment is defined as when the AOD of fine (coarse) aerosols exceeds 60% quantiles across all sampled data, ensuring that the AOD of fine (coarse) aerosols accounts for over 50% of total aerosols. Based on these standards, a coarse aerosol-polluted environment is classified as having a coarse AOD > 0.0425, where the proportion of coarse AOD to total aerosols exceeds 50%. Similarly, a fine aerosol-polluted environment is defined by a fine AOD > 0.315, with the proportion of fine AOD to total aerosols exceeding 50% (see Table 1 for reference). During the study period, there are 9237, 967, and 2986 shallow precipitation samples under clean, fine aerosol, and coarse aerosol-polluted conditions, respectively (Figure 1c). The shallow precipitation accounts for a higher proportion with respect to the total precipitation samples, reaching 8% in clean and fine aerosol-polluted conditions. However, under coarse aerosol-polluted conditions, the proportion of shallow precipitation samples is much lower, at around ~2%. Due to the lower AOD of coarse aerosol mode, occurrences where the AOD of coarse aerosols account for more than 50% of the total AOD are less

https://doi.org/10.5194/egusphere-2024-2206
Preprint. Discussion started: 14 August 2024

frequent, which explains the lower shallow precipitation samples in coarse aerosol-polluted conditions. However, the nearly 3000 samples ensure the reliability of our research results to some extent.

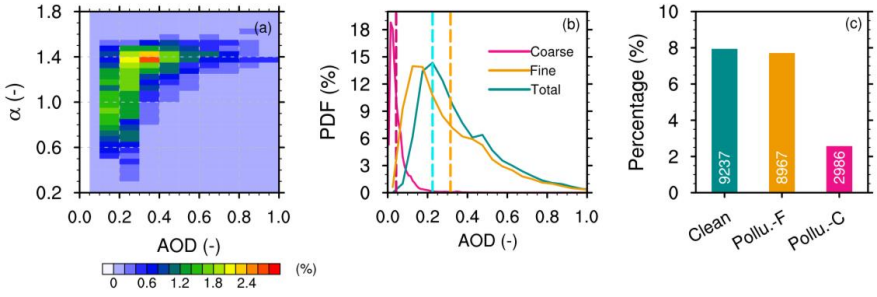

Figure 1 The countered frequency of AOD and α before the appearance of shallow precipitation (a), the probability distribution functions of AOD for fine, coarse and total aerosols before shallow precipitation event (b), the percentages of shallow precipitation samples to total precipitation samples in terms of different aerosol conditions (c) as observed by DPR in southern China during the summers of 2014-2021. The pink vertical line (orange) in (b) indicates the upper 60% for fine (coarse) aerosols, respectively. The cyan vertical line in (b) indicates the lower 30% for the total AOD. The shallow precipitation samples are indicated by white text in (c).

Table 1 Definitions of polluted and clean conditions of coarse and fine aerosol modes in southern China during the summers of 2014-2021.

Environment	Definition
Clean	Total AOD < 0.225
Polluted_Fine	Fine AOD > 0.315 & Fine AOD ratio>50%
Polluted_Coarse	Coarse AOD> 0.0425 and Coarse AOD > 0.0425 & Coarse AOD ratio>50%

https://doi.org/10.5194/egusphere-2024-2206
Preprint. Discussion started: 14 August 2024

3 Results

3.1 Influence of aerosol on rainfall and microphysical characteristics

Figure 2 presents boxplots of near-surface RR, N_w, D_m and Z_e at 2.5 km in altitude, as well as LWP and STH for shallow precipitation under different aerosol conditions in South China. Compared to the clean environment, the RR decreases slightly in the fine aerosol-polluted environment, with a median value of only 0.7 mm h^{-1}, while in the coarse aerosol-polluted environment, the median value of RR increases, reaching 1.0 mm h^{-1}. This is consistent with a higher median Z_e at 2.5 km in altitude (25 dBZ) under coarse aerosol-polluted conditions and a lower one (22 dBZ) under fine aerosol-polluted conditions, suggesting the inhibition effect of fine particles and the invigoration effect of coarse particles on the near-surface RR for shallow precipitation. However, the coarse aerosol-polluted environment is not promoting vertical development of shallow precipitation clouds (Figure 2f), with a significantly lower median STH (~3.2 km) than that (~3.7 km) in fine aerosol-polluted environments. From a microphysical perspective, compared to the clean environment, the median values of LWP (with a median of approximately 170 g m^{-2}), N_w (34), and D_m (1.05 mm) at 2.5 km altitude decrease under the fine aerosol-polluted mode. On the contrary, under coarse aerosol-polluted conditions, the median values of LWP, N_w, and D_m at 2.5 km altitude increase, reaching 210 g m^{-2}, 35, and 1.15 mm, respectively. This indicates that the enhancement of near-surface RR under coarse aerosol-polluted conditions is contributed by high concentrations of large rain droplets, while the weakening under fine aerosol-polluted conditions is influenced by low concentrations of small rain droplets. In South China, sea salt aerosols are the primary components of coarse particles, and a recent study by Liu et al. (2022) has shown that sea salt aerosols are more likely to form large cloud droplets through hygroscopic growth, which are more likely to form rain droplets through condensation and other microphysical processes, resulting in higher cloud water content within shallow precipitation clouds. On the

https://doi.org/10.5194/egusphere-2024-2206
Preprint. Discussion started: 14 August 2024

contrary, fine mode aerosols tend to reduce the effective radius of cloud droplets, with small cloud droplets being prone to evaporation and subsequent loss of cloud water. Our results fill the gap between cloud microphysics, precipitation microphysics, and precipitation.

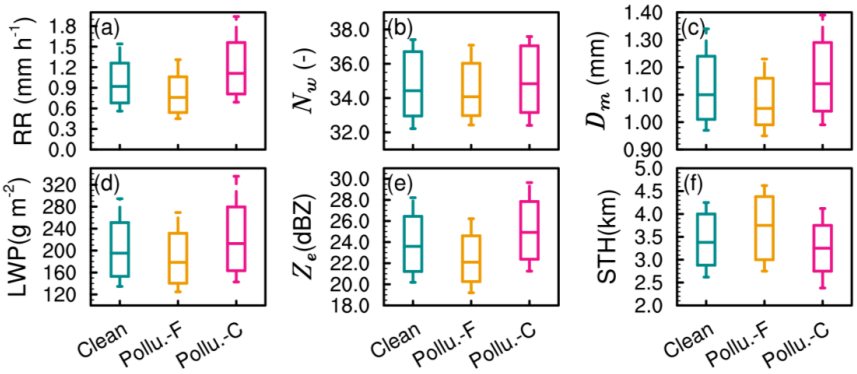

Figure 2 The box plot of the near-surface rain rate (a), N_w (b), D_m (c), LWP (d), Z_e (e) and STH (f) for shallow precipitation under different aerosol conditions in southern China during the summers of 2014-2021. The upper and lower edges of the boxes represent the lower and upper tritile, respectively. The line in the box is the median. The lower quartile and the upper quartile are shown by the whiskers that extend from the box.

DSDs directly impact RR. Therefore, the DSDs at 2.5 km altitude for shallow precipitation clouds over southern China under three aerosol conditions are illustrated in Figure 3. Regardless of aerosol background, DSDs exhibit characteristics of high concentrations of small particles and low concentrations of large particles, consistent with previous research findings (Wang et al., 2016; Chen et al., 2022). In a clean environment (Figure 3a), the DSD of shallow precipitation exhibits a high-frequency center around N_w of approximately 40, with D_m around 1.0 mm, reaching a frequency

https://doi.org/10.5194/egusphere-2024-2206
Preprint. Discussion started: 14 August 2024

exceeding 70%. A secondary peak (40%) slightly shifts towards the lower right, located at D_m around 1.2 mm and N_w around 32. In the case of fine aerosol-polluted environments (Figure 3b), the average RR (1.15 mm h^{-1}) and D_m (1.14 mm) are slightly reduced compared to the clean environment, while the mean N_w *increases* slightly to 36.37. Furthermore, the secondary peak observed in a clean environment becomes more pronounced under fine aerosol-polluted conditions, with a frequency exceeding 50%. In contrast to clean and fine aerosol-polluted environments, both the mean values of RR and N_w increase under coarse aerosol-polluted conditions (Figure 3c). Furthermore, the DSD reveals more samples with D_m exceeding 2 mm or N_w exceeding 40, further indicating the enhancement of RR for shallow precipitation in coarse aerosol-polluted environments.

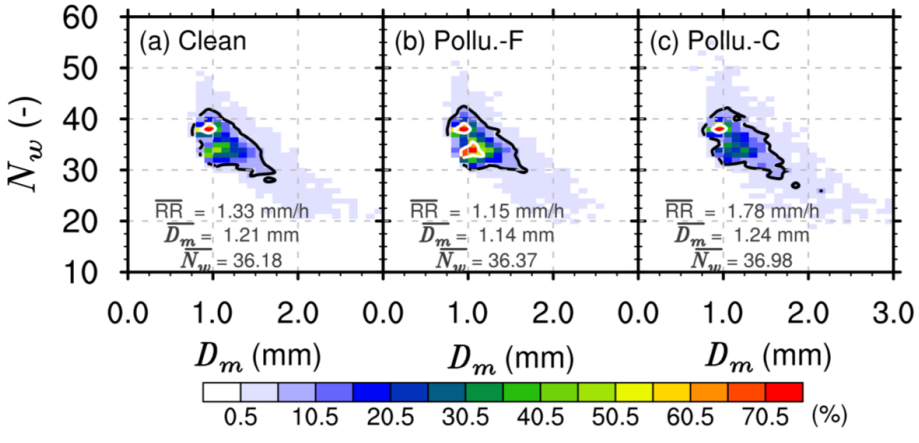

Figure 3 DSDs at 2.5 km altitude for shallow precipitation in clean (a), fine (b) aerosol-polluted and coarse (c) aerosol-polluted environments over southern China during the summers of 2014-2021. The mean values of D_m and N_w under different aerosol conditions are presented in each panel. The 5% and 50% contours are indicated by black and white solid lines, respectively.

https://doi.org/10.5194/egusphere-2024-2206
Preprint. Discussion started: 14 August 2024

3.2 Influence of aerosol on microphysical structures and processes

The above analysis has shown significant differences in near-surface RR and DSD for shallow precipitation under different aerosol environments. The vertical structure of precipitating clouds is closely related to near-surface RR and DSD, reflecting the thermal and dynamic structure within the clouds. Investigating the precipitation and microphysical structures under different aerosol backgrounds can further deepen our understanding of the thermodynamic and microphysical mechanisms by which aerosols affect shallow precipitation near the surface.

Figure 4 presents the profiles of the median values of Z_e, RR, D_m, and N_w for shallow precipitation over southern China in summer in three different aerosol environments. Overall, shallow precipitation shows an increase in Z_e, RR, D_m, and N_w with decreasing altitude under different aerosol backgrounds, indicating that the shallow precipitation growth process is mainly dominated by warm rain collision-coalescence processes. This is similar to the precipitation structures for shallow precipitation in the Yangtze-Huaihe River Basin (Chen et al., 2024). However, the median values of Z_e, RR, D_m, and N_w at each altitude differ under different aerosol environments. The promotion effect of coarse aerosols and the inhibition effect of fine aerosols are present throughout the profile. For example, the median values of Z_e, RR, D_m, and N_w at any given altitude are the largest in a coarse aerosol-polluted environment and the smallest in a fine aerosol-polluted pollution. Furthermore, the most significant differences in precipitation microphysical structures under different aerosol backgrounds occur near the surface (below 2 km). For example, at 1 km altitude, the differences in Z_e, RR, D_m, and N_w are approximately 3 dBZ, 0.4 mm h^{-1}, 0.12 mm and 1, respectively.

Taking into account the increasing amplitude of the median values of Z_e, RR, D_m, and N_w with decreasing altitude, there are significant differences under different aerosol backgrounds, reflecting different microphysical precipitation processes within shallow precipitation systems. Specifically, in coarse aerosol-polluted environments, the

https://doi.org/10.5194/egusphere-2024-2206
Preprint. Discussion started: 14 August 2024

increases in Z_e, RR, D_m, and N_w within the same altitude layer are the largest, while the increases in these variables are the smallest in fine aerosol-polluted environments. This explains why an increase in coarse particles enhances RR compared to that in a clean environment, while an increase in fine aerosols inhibits precipitation. For example, the median D_m in clean environments increase from 1.07 mm at 3 km altitude to 1.1 mm at 1 km altitude. In coarse aerosol-polluted environments, D_m shows a more significant increasing trend, with the median D_m increasing from 1.08 mm at 3 km to 1.14 mm at 1 km. However, in fine aerosol-polluted environments, the increase in the median D_m from 3 km to 1 km is weak, almost remaining constant at around 1.04 mm.

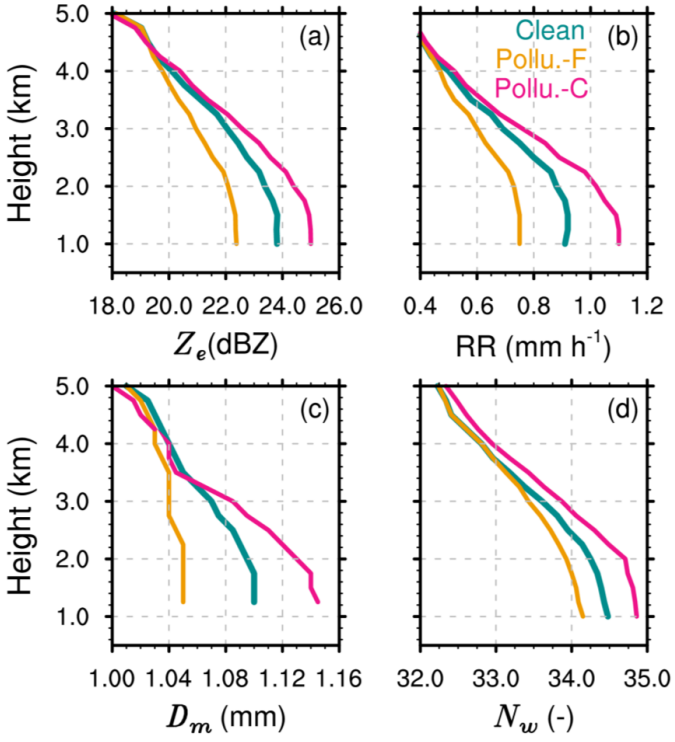

Figure 4 The profiles of the median Z_e (a), rain rate (b), D_m (c), and N_w (d) for shallow precipitation in different aerosol conditions over southern China during the summers of 2014-2021.

https://doi.org/10.5194/egusphere-2024-2206
Preprint. Discussion started: 14 August 2024

To more intuitively reflect the potential impact of different types of aerosol on the near-surface microphysical processes of shallow precipitation, the methods of Kumjian et al. (2014) are adopted to quantify the near-surface microphysical processes using changes in Z_e ($\Delta Z_e = Z_e^{1km} - Z_e^{3km}$) and D_m ($\Delta D_m = D_m^{1km} - D_m^{3km}$) at 3 km and 1 km. For example, collision-coalescence typically causes increases in Z_e and D_m, while breakup causes decreases. Likewise, an increase in D_m and a decrease in Z_e toward the ground (positive ΔD_m and negative ΔZ_e) signify that the governing process is evaporation or size sorting. The fingerprint of a "balance" between collision-coalescence and breakup is indicated by a slight decrease in D_m and an increase in Z_e.

Figure 5 shows the proportions of collision-coalescence, size sorting, breakup, and balance processes of raindrop particles in shallow precipitation clouds under three different aerosol backgrounds. In general, the microphysical process of collision-coalescence of hydrometeors dominates shallow precipitation, accounting for more than 60%. This is followed by the hydrometeor breakup process, which accounts for more than 20%, while size sorting and balance processes account for the smallest proportions, only about 3% and 1%, respectively. In fine mode aerosol-polluted environments, the proportion of the collision-coalescence process is only 62.4%, while this proportion reaches 74.1% in coarse aerosol-polluted environments, with an increase of about 11.7%. Similarly, the proportion of the hydrometeor particle breakup process is 33.1% in fine aerosol-polluted environments and 22.1% in fine aerosol-polluted environments (a decrease of 10%). This indicates the increase in the proportion of raindrop breakup processes and the weakening of the collision-coalescence process in fine aerosol-polluted environments, which may be the reason for the weakened near-surface RR. Conversely, in coarse aerosol-polluted mode environments, raindrop hydrometeors undergo more collision-coalescence growth processes and fewer breakup and evaporation processes, which contributes to the enhancement of surface RR.

https://doi.org/10.5194/egusphere-2024-2206
Preprint. Discussion started: 14 August 2024

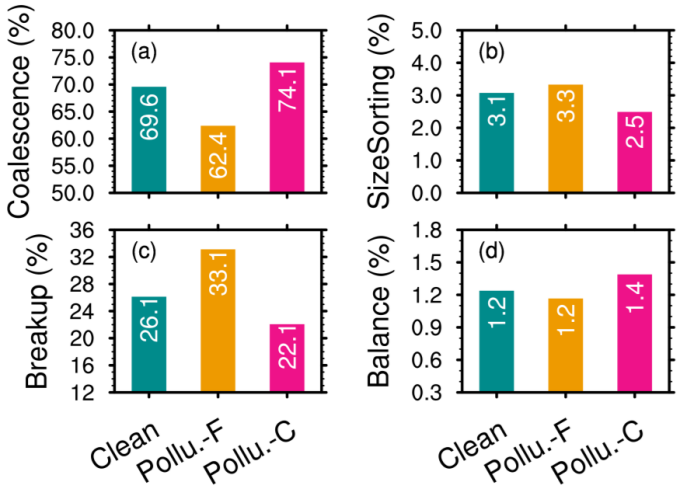

Figure 5 The percentages of coalescence (a), size sorting (b), break-up(c), and balance (d) for shallow precipitation shallow precipitation rain hydrometeors under different aerosol conditions in southern China during the summers of 2014-2021.

3.3 Sensitivities of aerosol impacts on precipitation to meteorological factors

The previous section results indicate that shallow precipitation under different aerosol backgrounds exhibits significant differences in surface RR, precipitation structures, and microphysical processes. However, precipitation itself is also influenced by thermal and dynamic environmental factors. Therefore, CAPE and RH at 850 hPa, which, respectively, reflect atmospheric instability and moisture, are used to isolate and assess the impact of aerosols. CAPE is divided into three intervals based on the terciles of CAPE values during precipitation events in southern China. CAPE 333 J kg^{-1} (CAPE1), 333 < CAPE < 1031 J kg^{-1} (CAPE2), and CAPE 1031 J kg^{-1} (CAPE3). Similarly, RH at 850 hPa is divided into three intervals, that is, RH 83% (RH1), 83% < RH < 91% (RH2), and RH 91% (RH3).

The box plots of RR, LWP and STH, as well as N_w, D_m, and Z_e at 2.5 km altitude

https://doi.org/10.5194/egusphere-2024-2206
Preprint. Discussion started: 14 August 2024

for shallow precipitation in southern China under different aerosol backgrounds and CAPEs are presented in Figure 6. Consistent with the conclusions of Figure 2, it is observed that under different CAPE conditions, the median STH of shallow precipitation clouds is the lowest in coarse aerosol-polluted environments, but the median RR and Z_e at 2.5 km are the highest. On the contrary, the median STH is the highest, but the median RR and Z_e at 2.5 km are the lowest in a fine aerosol-polluted environment. This indicates that the suppression of RR in fine aerosol-polluted environments and the invigoration of RR in coarse aerosol-polluted environments are independent of the dynamic conditions (CAPE in this case). Furthermore, when seen from microphysics, under different CAPE conditions, shallow precipitation clouds in coarse aerosol-polluted environments exhibit the highest median values of values of LWP, N_w, and D_m at 2.5 km, while these variables are the lowest in fine aerosol-polluted environments. This helps explain why shallow precipitation has the highest near-surface RR in coarse aerosol-polluted environments and the lowest surface RR in fine aerosol-polluted environments from the microphysical perspective.

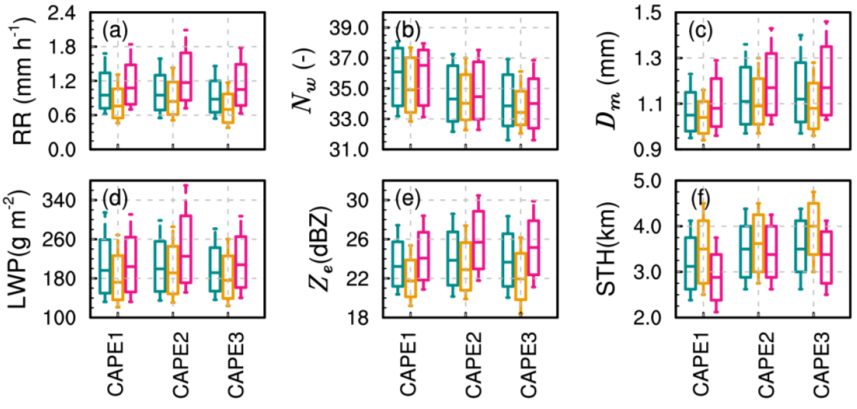

Figure 6 Box plot of the near-surface rain rate (a), N_w (b), D_m (c), LWP (d), Z_e (e), and STH (f) under different aerosol and CAPE conditions for shallow precipitation over southern China during the summers of 2014-2021. The upper and lower edges of the boxes represent the lower and upper tritile, respectively. The line in the box is the

https://doi.org/10.5194/egusphere-2024-2206
Preprint. Discussion started: 14 August 2024

409 median. The lower quartile and the upper quartile are shown by the whiskers that extend
410 from the box.
411
412 Similarly, the sensitivity of humidity to the impact of aerosol on shallow
413 precipitation is examined by presenting the box plots of precipitation parameters, as
414 illustrated in Figure 7. Regardless of 850hPa-RH, the vertical development of shallow
415 precipitation clouds is hindered in coarse aerosol-polluted environments, with the
416 median STH being the smallest. However, the near-surface RR is the highest,
417 corresponding to the highest median Z_e at 2.5 km. On the contrary, in fine particle
418 pollution environments, the vertical development of shallow precipitation clouds is
419 enhanced (with the highest median STH), but the near-surface RR and Z_e are the
420 weakest. This further confirms that the impact of coarse and fine aerosol particles on
421 near-surface RR and LWP is independent of moisture and dynamic conditions.
422 It is important to note that the degree of enhancement or suppression of RR by
423 coarse and fine aerosols varies under different humidity conditions. Compared to high-
424 humidity environments, coarse aerosols have the most significant enhancement effect
425 on RR, while fine aerosols have the most significant suppression effect in relatively
426 low-humidity environments (RH1). In fine aerosol-polluted environments, the box plot
427 of RR shows a significant decrease compared to that in clean environments, while the
428 coarse aerosol-polluted environment shows a significant increase. Specifically, the
429 median RR in the coarse aerosol-polluted environment is around 1.1 mm h^{-1}, whereas
430 it is around 0.7 mm h^{-1} in the fine aerosol-polluted environment.
431 Regarding STH, under low relative humidity and fine aerosol pollution conditions,
432 shallow precipitation clouds develop more deeply, with the 25th percentile of STH
433 reaching 5 km, significantly higher than in clean and coarse aerosol-polluted
434 environments. This may be because there is a reduction in the effective radius of cloud
435 droplets in fine aerosol-polluted and low-humidity conditions. Smaller cloud droplets
436 are more prone to evaporation, resulting in lower LWP, which does not favor an increase
437 in near-surface RR. This is also reflected in the near-surface DSD, which is

https://doi.org/10.5194/egusphere-2024-2206
Preprint. Discussion started: 14 August 2024

characterized by lower N_w and smaller D_m. However, although the humidity is relatively low, the coarse particles, being more hygroscopic, can form larger cloud droplets, reducing the loss of cloud water due to evaporation (resulting in higher LWP), and thereby enhancing surface RR. This is also reflected in the near-surface DSD, which is characterized by higher N_w and larger D_m. In high-humidity environments, a high concentration of fine particles can promote the formation of more cloud condensation nuclei, which to some extent reduces the loss of cloud water due to the evaporation of small particles. Therefore, the LWP in fine particle pollution environments does not differ much from that in coarse aerosol-polluted environments. This may further lead to smaller differences in RR, Z_e, and other variables between coarse and fine aerosol-polluted environments in relatively high humidity conditions.

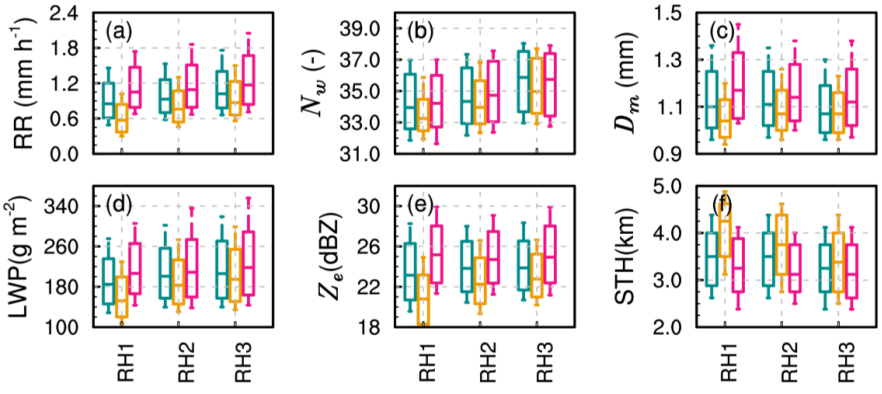

Figure 7 Same as Figure 6, but for RH at 850hPa.

3.4 Sensitivities of aerosol impacts on microphysical structures and processes to meteorological factors

This section continues to explore the impact of coarse and fine aerosols on

https://doi.org/10.5194/egusphere-2024-2206
Preprint. Discussion started: 14 August 2024

precipitation structures and microphysical processes under different environmental conditions. As shown in Figure 8, under different CAPE and aerosol backgrounds, shallow precipitation profiles consistently exhibit increasing trends in Z_e, RR, N_w, and D_m with decreasing altitude. Moreover, regardless of the CAPE conditions, at a given altitude, Z_e and RR are the highest in coarse aerosol-polluted environments, followed by a clean environment, and the lowest in fine aerosol-polluted environments. This is consistent with the results in Figure 4. When compared between different CAPE conditions, the Z_e, RR, and D_m of shallow precipitation in CAPE2 are the highest at different altitudes, while as the CAPE increases further (CAPE3), these values even decrease. Apart from instability, precipitation can be influenced by moisture, topography, and other factors; therefore, it is possible for an even lower RR in high CAPE conditions.

When seen from D_m and N_w (Figures 8c1-c3, d1-d3), the promotion effect of coarse aerosols and the suppression effect of fine aerosols can vary under different dynamic environmental conditions. Under moderate CAPE conditions (CAPE2), D_m and N_w in coarse aerosol-polluted environments are the largest at different altitudes, while D_m and N_w in a fine aerosol-polluted environment are the smallest. This indicates that under moderate CAPE conditions, the enhancement of RR in coarse aerosol-polluted environments is contributed by large particles and high concentrations. For low CAPE conditions (CAPE1), the median D_m above 3 km is even the smallest in coarse aerosol-polluted environments, compared to clean and fine aerosol-polluted environments. Therefore, the maximum values of RR and Z_e at this layer are mainly contributed by high concentrations of raindrop particles (with large median N_w, as shown in Figure 8d-1). For high CAPE conditions (CAPE3), the median N_w above the 3 km altitude layer in coarse aerosol-polluted environments is even the smallest. Therefore, the maximum values of RR and Z_e at this altitude are mainly contributed by high concentrations of raindrop particles (with large median D_m, as shown in Figure 8c-3).

https://doi.org/10.5194/egusphere-2024-2206
Preprint. Discussion started: 14 August 2024

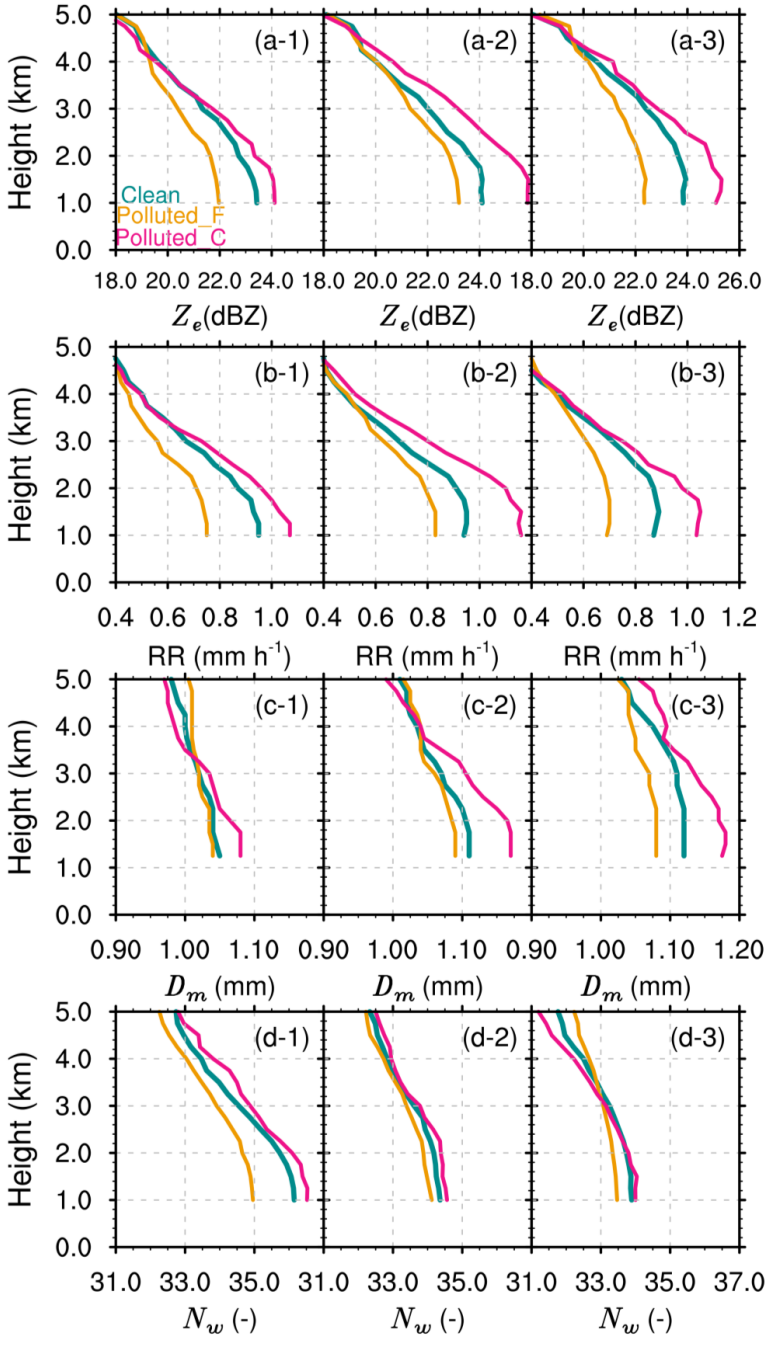

485

486 **Figure 8** The Z_e (a), rain rate (b), D_m (c), and N_w (d) profiles for shallow precipitation

487 in different aerosol and CAPE conditions over southern China during the summers of

https://doi.org/10.5194/egusphere-2024-2206
Preprint. Discussion started: 14 August 2024

2014-2021. CAPE1, CAPE2, and CAPE3 are shown in the left, middle, and right panels, respectively.

Similarly, the profiles of Z_e, RR, D_m, and N_w in different 850hPa-RH and aerosol backgrounds are illustrated in Figure 9. Consistent with previous research results, the median values of Z_e, RR, D_m, and N_w of shallow precipitation exhibit a gradual increase with decreasing altitude, reflecting the warm rain collision-coalescence growth process. However, the microphysical structures of shallow precipitation vary under different RH conditions with similar aerosol backgrounds. As RH at 850hPa increases, the median values of Z_e, RR, D_m, and N_w of shallow precipitation increase more significantly with decreasing altitude. For example, under low humidity conditions (RH1), the median D_m increases slightly when hydrometeors fall from 3 km to 1 km (Figure 9c-1), and even decreases under fine aerosol-polluted conditions, indicating more breakup processes. Subsequently, with increasing humidity, the increase in D_m becomes more apparent (Figure 9c-3). For example, where the median D_m increases from 1.05 mm to 1.15 mm in coarse aerosol-polluted environments.

When compared among different aerosol backgrounds, the median values of Z_e and RR in coarse aerosol-polluted environments are much larger at each altitude layer and have greater increases with decreasing altitude. Conversely, under fine aerosol-polluted conditions, the median Z_e and RR values are the smallest at each altitude layer, with the smallest increases with decreasing altitude. This is consistent with previous conclusions (Figures 4 and 8), further indicating that the impact of coarse and fine aerosols on the near-surface RR and the precipitation structure is not sensitive to dynamic and moisture conditions. However, from a microphysical structure perspective, there are still some differences in aerosol backgrounds. Under low and moderate humidity conditions (RH1 and RH2), at a given altitude, D_m and N_w are the largest in coarse aerosol-polluted environments and the smallest in fine aerosol-polluted environments. However, under RH3 conditions, in the same altitude layer, N_w is the largest and D_m is relatively small in a clean environment; N_w is moderate and D_m is the largest in coarse aerosol-polluted environments; and N_w is the smallest and D_m is relatively small in fine aerosol-polluted environments. This indicates that in high RH environments, fine aerosols mainly reduce RR by suppressing the concentration of raindrops, while coarse aerosols increase RR by increasing the size of hydrometeors. Furthermore, the differences in precipitation structures in aerosol-polluted coarse and

https://doi.org/10.5194/egusphere-2024-2206
Preprint. Discussion started: 14 August 2024

fine environments depend on humidity conditions, consistent with the conclusions in Figure 7. The differences are the greatest under RH1 conditions, with the differences in RR, Z_e, D_m, and N_w at 1 km altitude being 0.42 mm h^{-1}, 4.5 dBZ, 0.19 mm, and about 1.3, respectively. Under RH3 conditions, the differences are smallest, with the differences in the aforementioned variables being 0.35 mm h^{-1}, 2 dBZ, 0.05 mm, and approximately 0.8, respectively.

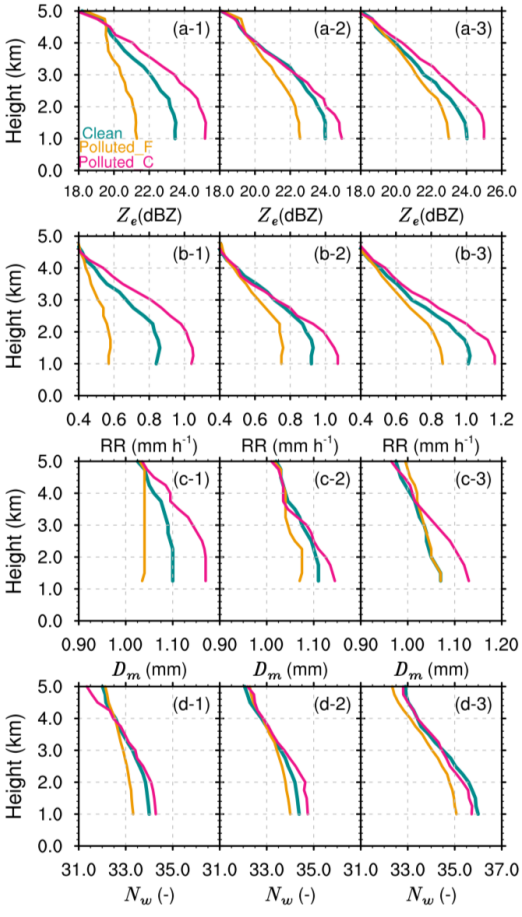

Figure 9 The Z_e (a), rain rate (b), D_m (c), and N_w (d) profiles for shallow precipitation in different aerosol conditions and 850 hPa-RH over southern China during the summers of 2014-2021. RH1, RH2, and RH3 are shown in left, middle, and right panels, respectively.

https://doi.org/10.5194/egusphere-2024-2206
Preprint. Discussion started: 14 August 2024

To quantitatively analyze the dependence of microphysical processes on dynamics and moisture under different aerosol backgrounds, we examined the differences in the two primary microphysical processes, i.e., collision-coalescence and breakup. As a result of the low proportions of size sorting and balance, further analysis of these microphysical processes is not included. The microphysical processes of precipitation depend on the dynamic and moisture conditions. For instance, with decreasing CAPE and increasing RH, the proportion of collision-coalescence increases, while the proportion of breakup decreases in clean, coarse, and fine aerosol-polluted environments. High RH and low CAPE environments favor aerosol particles in the boundary layer collecting moisture to form more cloud droplets, which further condense to form more raindrops, thereby promoting the collision-coalescence process.

When different aerosol backgrounds are compared, we can identify some general patterns that are independent of thermodynamic conditions. First, regardless of CAPE, RH or aerosol background, shallow precipitation systems are dominated by the warm rain collision-coalescence process, with a proportion ranging from a minimum of 51.2% to a maximum of 82.3%. There is also a certain proportion of break-up processes, ranging from 14.6% to 43.2%. Second, regardless of the presence of CAPE and RH, the proportion of the collision-coalescence process is always the highest in coarse aerosol-polluted environments, while the proportion of the breakup process is always the highest in fine aerosol-polluted environments. These conclusions are consistent with previous findings. However, the increase in the proportion of collision coalescence in coarse aerosol-polluted environments and the increase in the proportion of breakup in fine aerosol-polluted environments depend on dynamic and moisture conditions. For example, under low relative humidity (RH1) conditions, the proportion of the collision-coalescence process in coarse aerosol-polluted environments (73.4%) is significantly higher than that in fine aerosol-polluted environments (51.2%). On the contrary, the proportion of the breakup process in fine aerosol-polluted environments (43.2%) is significantly higher than in coarse aerosol-polluted environments (22.3%). This is consistent with previous findings that under RH1 conditions, D_m in fine aerosol-polluted environments rapidly decreases with decreasing altitude.

https://doi.org/10.5194/egusphere-2024-2206
Preprint. Discussion started: 14 August 2024

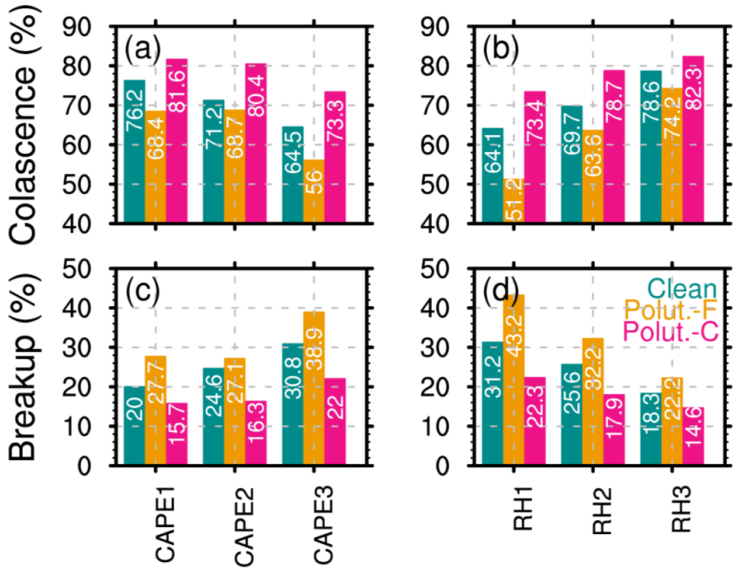

Figure 10 The percentages of coalescence (a), size sorting (b), break-up(c), and balance (d) for shallow precipitation rain hydrometeors under different aerosol conditions in southern China during the summers of 2014-2021.

4 Conclusion and Discussion

Using the combined data of DPR, MERRA-2 aerosol datasets, and ERA5 during the summers of 2014-2021, this study investigates the potential impacts of coarse and fine aerosols on the RR, microphysical structure, and processes for shallow precipitation in South China. Clean, coarse, and fine aerosol-polluted environments are classified according to the AOD for total aerosols, coarse aerosols, and fine aerosols derived from MERRA-2. The ERA5 reanalysis data is used to explore the sensitivity of aerosol impacts on shallow precipitation to dynamic and moisture conditions in South China. The main findings are summarized as follows.

Compared to clean environments, coarse aerosol-polluted environments promote near-surface RR of shallow precipitation, characterized by stronger near-surface RR (average precipitation intensity of 1.78 mm h^{-1}), higher concentrations (average N_w =

https://doi.org/10.5194/egusphere-2024-2206
Preprint. Discussion started: 14 August 2024

36.98) and larger raindrop sizes (average D_m = 1.24 mm) of hydrometeor particles. This may be attributed to the significant proportion of sea salt particles in the coarse particles in South China, which tend to form larger cloud droplets through hygroscopic growth, leading to larger raindrop particles through microphysical processes such as condensation. On the contrary, fine aerosol-polluted environments suppress near-surface RR, with an average near-surface RR of only 1.33 mm h^{-1} and lower concentrations and smaller sizes of hydrometeors (average N_w = 36.37, average D_m = 1.14 mm). However, fine aerosol-polluted environments favor the vertical development of shallow precipitation clouds (median STH of 3.7 km), approximately 0.5 km higher than in coarse aerosol-polluted conditions.

From the perspective of precipitation vertical structure and microphysical processes, shallow precipitation is dominated by warm-rain collision-coalescence processes under different aerosol backgrounds, with the collision-coalescence process accounting for over 62%. However, there are significant differences in the efficiency of hydrometeor collision-coalescence growth under different aerosol backgrounds. Compared to clean environments, the median values of Z_e, RR, D_m, and N_w are highest in conditions contaminated with coarse aerosols and lowest in conditions contaminated with fine aerosols at all altitude levels. When seen from the microphysical processes, the increase in D_m with decreasing altitude is most pronounced under coarse aerosol-polluted conditions, reflecting more significant collision-coalescence growth processes, accounting for 74.1%. In contrast, the increase in D_m with decreasing altitude is weakest under fine aerosol-polluted conditions, due to the higher proportion of breakup processes (accounting for 33.1%) and a decrease of approximately 12% in the collision-coalescence process (accounting for 62.4%).

The promotion of RR associated with more significant collision-coalescence processes by coarse aerosols, as well as the suppression of RR characterized by more significant breakup processes by fine aerosols are independent of CAPE and humidity conditions. However, the promotion and suppression effects are the most pronounced under low relative humidity conditions (RH1). For instance, the median RR is around

https://doi.org/10.5194/egusphere-2024-2206
Preprint. Discussion started: 14 August 2024

1.12 mm h^{-1} under coarse aerosol-polluted conditions, while it is around 0.7 mm h^{-1} under fine aerosol-polluted conditions, with a difference of approximately 0.42 mm h^{-1}. The collision-coalescence and breakup microphysical processes play an important role in these differences, with the collision-coalescence accounting for 73.4% under coarse aerosol-polluted conditions, significantly higher than 51.2% under fine aerosol-polluted conditions. Correspondingly, the breakup microphysical processes account for 43.2% under fine aerosol-polluted conditions, significantly higher than the 22.3% in coarse aerosol-polluted conditions. Under high relative humidity conditions, fine aerosol-polluted environments primarily reduce RR by inhibiting hydrometeor concentration (possibly as a result of the evaporation effects of small cloud droplets), while coarse aerosols invigorate RR by increasing the size of hydrometeor particles. Additionally, the increase in RR above 3 km in coarse aerosol-polluted environments is mainly driven by the high concentration of hydrometeors in low instability conditions, while by large hydrometeors in high instability environments.

Our results differ from previous findings, which suggest that increased aerosols under high relative humidity conditions inhibit precipitation (Li et al., 2011). This highlights the uniqueness of shallow precipitation and the differing impacts of various aerosol species on shallow precipitation. It is important to note that even though MERRA-2 is a relatively reliable dataset, there is an urgent need for long-term observational data on aerosol concentrations, as well as some numerical studies, to further validate our conclusions.

Data availability

The GPM DPR data provided by NASA Goddard Space Flight Center's Mesoscale Atmospheric Processes Laboratory and Precipitation Processing System (PPS) can be downloaded from https://pmm.nasa.gov/dataaccess/downloads/gpm. MERRA-2 data can be downloaded from https://gmao.gsfc.nasa.gov/reanalysis/MERRA-2/data_access/. The ERA5 data can be downloaded from https://www.ecmef.int/en/forecasts/dataset/ecmwf-reanalysis-v5. The ancillary digital

https://doi.org/10.5194/egusphere-2024-2206
Preprint. Discussion started: 14 August 2024

terrain data is from National Geophysical Data Center (NGDC) (available online at http://www.ngdc.noaa.gov, available on May 2023).

Author contributions

YY designed the manuscript and led the data analysis; FC performed the analysis and wrote the manuscript draft; YL and LY collected the data; GL, LY, and SL reviewed and edited the manuscript; SL helped with the data analysis.

Declaration of competing interest

The authors declare no competing interests.

Acknowledgments

The authors thank NASA Goddard Space Flight Center's Mesoscale Atmospheric Processes Laboratory and PPS, NGDC, and ECMWF for providing the analysis data.

Financial support

This work has been jointly supported by the China National Natural Science Foundation (grant 41805023), the Jiangsu Meteorological Bureau General Project (KM202407), the Open Grants of China Meteorological Administration Radar Meteorology Key Laboratory (2024LRM-B06), and the Open Project of KLME & CIC-FEMD (KLME202303).

Reference

Buchard, V., da Silva, A. M., Colarco, P. R., Darmenov, A., Randles, C. A., Govindaraju, R., Torres, O., Campbell, J., and Spurr, R.: Using the OMI aerosol index and absorption aerosol optical depth to evaluate the NASA MERRA Aerosol Reanalysis, Atmos. Chem. Phys., 15, 5743-5760, 10.5194/acp-15-5743-2015, 2015.

https://doi.org/10.5194/egusphere-2024-2206
Preprint. Discussion started: 14 August 2024

664 Buchard, V., Randles, C. A., da Silva, A. M., Darmenov, A., Colarco, P. R., Govindaraju, R., Ferrare,
665 R., Hair, J., Beyersdorf, A. J., Ziemba, L. D., and Yu, H.: The MERRA-2 Aerosol Reanalysis,
666 1980 Onward. Part II: Evaluation and Case Studies, Journal of Climate, 30, 6851-6872,
667 https://doi.org/10.1175/JCLI-D-16-0613.1, 2017.
668 Chen, F., Fu, Y., Liu, P., and Yang, Y.: Seasonal Variability of Storm Top Altitudes in the Tropics
669 and Subtropics Observed by TRMM PR, Atmospheric Research, 169, 113-126,
670 https://doi.org/10.1016/j.atmosres.2015.09.017, 2016.
671 Chen, F., Zheng, X., Wen, H., and Yuan, Y.: Microphysics of Convective and Stratiform
672 Precipitation during the Summer Monsoon Season over the Yangtze–Huaihe River Valley,
673 China, Journal of Hydrometeorology, 23, 239-252, 2022.
674 Chen, F., Zheng, X., Yu, L., Wen, H., and Liu, Y.: Precipitation, microphysical and environmental
675 characteristics for shallow and deep clouds over Yangtze-Huaihe River Basin, Atmospheric
676 Research, 298, 107155, https://doi.org/10.1016/j.atmosres.2023.107155, 2024.
677 Chen, Y., Zhang, A., Zhang, Y., Cui, C., Wan, R., Wang, B., and Fu, Y.: A Heavy Precipitation Event
678 in the Yangtze River Basin Led by an Eastward Moving Tibetan Plateau Cloud System in the
679 Summer of 2016, Journal of Geophysical Research: Atmospheres, 125, e2020JD032429,
680 https://doi.org/10.1029/2020JD032429, 2020.
681 Chin, M., Ginoux, P., Kinne, S., Torres, O., Holben, B. N., Duncan, B. N., Martin, R. V., Logan, J. A.,
682 Higurashi, A., and Nakajima, T.: Tropospheric Aerosol Optical Thickness from the GOCART
683 Model and Comparisons with Satellite and Sun Photometer Measurements, Journal of the
684 Atmospheric Sciences, 59, 461-483, https://doi.org/10.1175/1520-
685 0469(2002)059<0461:TAOTFT>2.0.CO;2, 2002.
686 Christensen, M. W. and Stephens, G. L.: Microphysical and macrophysical responses of marine
687 stratocumulus polluted by underlying ships: 2. Impacts of haze on precipitating clouds,
688 Journal of Geophysical Research: Atmospheres, 117, https://doi.org/10.1029/2011JD017125,
689 2012.
690 Fan, C., Wang, M., Rosenfeld, D., Zhu, Y., Liu, J., and Chen, B.: Strong Precipitation Suppression by
691 Aerosols in Marine Low Clouds, Geophysical Research Letters, 47, e2019GL086207,
692 https://doi.org/10.1029/2019GL086207, 2020.
693 Fan, J., Rosenfeld, D., Zhang, Y., Giangrande, S. E., Li, Z., Machado, L. A. T., Martin, S. T., Yang, Y.,
694 Wang, J., Artaxo, P., Barbosa, H. M. J., Braga, R. C., Comstock, J. M., Feng, Z., Gao, W.,
695 Gomes, H. B., Mei, F., Pöhlker, C., Pöhlker, M. L., Pöschl, U., and de Souza, R. A. F.:
696 Substantial convection and precipitation enhancements by ultrafine aerosol particles,
697 Science, 359, 411-418, 10.1126/science.aan8461, 2018.
698 Guo, J., Su, T., Chen, D., Wang, J., Li, Z., Lv, Y., Guo, X., Liu, H., Cribb, M., and Zhai, P.: Declining
699 Summertime Local-Scale Precipitation Frequency Over China and the United States, 1981–
700 2012: The Disparate Roles of Aerosols, Geophysical Research Letters, 46, 13281-13289,
701 https://doi.org/10.1029/2019GL085442, 2019.
702 Huang, H., Zhao, K., Fu, P., Chen, H., Chen, G., and Zhang, Y.: Validation of Precipitation
703 Measurements From the Dual-Frequency Precipitation Radar Onboard the GPM Core
704 Observatory Using a Polarimetric Radar in South China, IEEE Transactions on Geoscience
705 and Remote Sensing, 1-16, 10.1109/TGRS.2021.3118601, 2021.
706 Iguchi, T., Seto, S., Meneghini, R., Yoshida, N., Awaka, J., and Kubota, T.: GPM/DPR level-2
707 algorithm theoretical basis document, NASA Goddard Space Flight Center, Greenbelt, MD,

https://doi.org/10.5194/egusphere-2024-2206
Preprint. Discussion started: 14 August 2024

USA, Tech. Rep, 2017.

Jiang, M., Li, Z., Wan, B., and Cribb, M.: Impact of aerosols on precipitation from deep convective clouds in eastern China, Journal of Geophysical Research: Atmospheres, 121, 9607-9620, https://doi.org/10.1002/2015JD024246, 2016.

Koren, I., Dagan, G., and Altaratz, O.: From aerosol-limited to invigoration of warm convective clouds, Science, 344, 1143-1146, doi:10.1126/science.1252595, 2014.

Kumjian, M. R., Khain, A. P., Benmoshe, N., Ilotoviz, E., Ryzhkov, A. V., and Phillips, V. T. J.: The Anatomy and Physics of ZDR Columns: Investigating a Polarimetric Radar Signature with a Spectral Bin Microphysical Model, Journal of Applied Meteorology and Climatology, 53, 1820-1843, 10.1175/JAMC-D-13-0354.1, 2014.

Lang, F., Huang, Y., Protat, A., Truong, S. C. H., Siems, S. T., and Manton, M. J.: Shallow Convection and Precipitation Over the Southern Ocean: A Case Study During the CAPRICORN 2016 Field Campaign, Journal of Geophysical Research: Atmospheres, 126, e2020JD034088, https://doi.org/10.1029/2020JD034088, 2021.

Li, Z., Niu, F., Fan, J., Liu, Y., Rosenfeld, D., and Ding, Y.: Long-term impacts of aerosols on the vertical development of clouds and precipitation, Nature Geoscience, 4, 888-894, 10.1038/ngeo1313, 2011.

Liu, C. and Zipser, E.: Regional variation of morphology of organized convection in the tropics and subtropics, Journal of Geophysical Research: Atmospheres, 118, 453-466, https://doi.org/10.1029/2012JD018409, 2013.

Liu, C. and Zipser, E. J.: "Warm Rain" in the Tropics: Seasonal and Regional Distributions Based on 9 yr of TRMM Data, Journal of Climate, 22, 767-779, https://doi.org/10.1175/2008JCLI2641.1, 2009.

Liu, F., Mao, F., Rosenfeld, D., Pan, Z., Zang, L., Zhu, Y., Yin, J., and Gong, W.: Opposing comparable large effects of fine aerosols and coarse sea spray on marine warm clouds, Communications Earth & Environment, 3, 232, 10.1038/s43247-022-00562-y, 2022.

Lolli, S., Sicard, M., Amato, F., Comeron, A., Gíl-Diaz, C., Landi, T. C., Munoz-Porcar, C., Oliveira, D., Dios Otin, F., Rocadenbosch, F., Rodriguez-Gomez, A., Alastuey, A., Querol, X., and Reche, C.: Climatological assessment of the vertically resolved optical and microphysical aerosol properties by lidar measurements, sunphotometer, and in-situ observations over 17 years at UPC Barcelona, EGUsphere, 2023, 1-29, 10.5194/egusphere-2023-893, 2023.

Miltenberger, A. K., Field, P. R., Hill, A. A., Rosenberg, P., Shipway, B. J., Wilkinson, J. M., Scovell, R., and Blyth, A. M.: Aerosol–cloud interactions in mixed-phase convective clouds – Part 1: Aerosol perturbations, Atmos. Chem. Phys., 18, 3119-3145, 10.5194/acp-18-3119-2018, 2018.

Molod, A., Takacs, L., Suarez, M., and Bacmeister, J.: Development of the GEOS-5 atmospheric general circulation model: evolution from MERRA to MERRA2, Geosci. Model Dev., 8, 1339-1356, 10.5194/gmd-8-1339-2015, 2015.

Ou, Y., Li, Z., Chen, C., Zhang, Y., Li, K., Shi, Z., Dong, J., Xu, H., Peng, Z., Xie, Y., and Luo, J.: Evaluation of MERRA-2 Aerosol Optical and Component Properties over China Using SONET and PARASOL/GRASP Data, Remote Sensing, 14, 821, 2022.

Radhakrishna, B., Satheesh, S., Narayana Rao, T., Saikranthi, K., and Sunilkumar, K.: Assessment of DSDs of GPM-DPR with ground-based disdrometer at seasonal scale over Gadanki, India, Journal of Geophysical Research: Atmospheres, 121, 2016.

https://doi.org/10.5194/egusphere-2024-2206
Preprint. Discussion started: 14 August 2024

Randles, C. A., Da Silva, A. M., Buchard, V., Colarco, P. R., Darmenov, A., Govindaraju, R., Smirnov, A., Holben, B., Ferrare, R., Hair, J., Shinozuka, Y., and Flynn, C. J.: The MERRA-2 Aerosol Reanalysis, 1980 - onward, Part I: System Description and Data Assimilation Evaluation, J Clim, 30, 6823-6850, 10.1175/jcli-d-16-0609.1, 2017.

Rosenfeld, D., Lohmann, U., Raga, G. B., O'Dowd, C. D., Kulmala, M., Fuzzi, S., Reissell, A., and Andreae, M. O.: Flood or Drought: How Do Aerosols Affect Precipitation?, Science, 321, 1309-1313, 10.1126/science.1160606, 2008.

Short, D. A. and Nakamura, K.: TRMM Radar Observations of Shallow Precipitation over the Tropical Oceans, Journal of Climate, 13, 4107-4124, https://doi.org/10.1175/1520-0442(2000)013<4107:TROOSP>2.0.CO;2, 2000.

Smalley, K. M. and Rapp, A. D.: The Role of Cloud Size and Environmental Moisture in Shallow Cumulus Precipitation, Journal of Applied Meteorology and Climatology, 59, 535-550, https://doi.org/10.1175/JAMC-D-19-0145.1, 2020.

Sun, E., Xu, X., Che, H., Tang, Z., Gui, K., An, L., Lu, C., and Shi, G.: Variation in MERRA-2 aerosol optical depth and absorption aerosol optical depth over China from 1980 to 2017, Journal of Atmospheric and Solar-Terrestrial Physics, 186, 8-19, https://doi.org/10.1016/j.jastp.2019.01.019, 2019a.

Sun, E., Che, H., Xu, X., Wang, Z., Lu, C., Gui, K., Zhao, H., Zheng, Y., Wang, Y., Wang, H., Sun, T., Liang, Y., Li, X., Sheng, Z., An, L., Zhang, X., and Shi, G.: Variation in MERRA-2 aerosol optical depth over the Yangtze River Delta from 1980 to 2016, Theoretical and Applied Climatology, 136, 363-375, 2019b.

Sun, N., Fu, Y., Zhong, L., and Li, R.: Aerosol effects on the vertical structure of precipitation in East China, npj Climate and Atmospheric Science, 5, 60, 10.1038/s41612-022-00284-0, 2022.

Sun, Y. and Zhao, C.: Distinct impacts on precipitation by aerosol radiative effect over three different megacity regions of eastern China, Atmos. Chem. Phys., 21, 16555-16574, 10.5194/acp-21-16555-2021, 2021.

Wang, M., Zhao, K., Xue, M., Zhang, G., Liu, S., Wen, L., and Chen, G.: Precipitation microphysics characteristics of a Typhoon Matmo (2014) rainband after landfall over eastern China based on polarimetric radar observations, Journal of Geophysical Research: Atmospheres, 121, 2016.

Xiao, Z., Zhu, S., Miao, Y., Yu, Y., and Che, H.: On the relationship between convective precipitation and aerosol pollution in North China Plain during autumn and winter, Atmospheric Research, 271, 106120, https://doi.org/10.1016/j.atmosres.2022.106120, 2022.

Yang, Y., Wang, R., Chen, F., Liu, C., Bi, X., and Huang, M.: Synoptic weather patterns modulate the frequency, type and vertical structure of summer precipitation over Eastern China: A perspective from GPM observations, Atmospheric Research, 249, 105342, https://doi.org/10.1016/j.atmosres.2020.105342, 2021.

Yuan, T., Remer, L. A., Pickering, K. E., and Yu, H.: Observational evidence of aerosol enhancement of lightning activity and convective invigoration, Geophysical Research Letters, 38, https://doi.org/10.1029/2010GL046052, 2011.

Zhang, A., Chen, Y., Zhang, X., Zhang, Q., and Fu, Y.: Structure of Cyclonic Precipitation in the Northern Pacific Storm Track Measured by GPM DPR, Journal of Hydrometeorology, 21, 227-240, https://doi.org/10.1175/JHM-D-19-0161.1, 2020a.

https://doi.org/10.5194/egusphere-2024-2206
Preprint. Discussion started: 14 August 2024

796 Zhang, Y., Yu, F., Luo, G., Chen, J.-P., and Chou, C. C. K.: Impact of Mineral Dust on Summertime
797 Precipitation Over the Taiwan Region, Journal of Geophysical Research: Atmospheres, 125,
798 e2020JD033120, https://doi.org/10.1029/2020JD033120, 2020b.

799